Cancelling Co-Channel Interference in Extremely Broadband Receivers

Ara Abdulsatar Assim [1,*], Aarno Pärssinen [2], and Timo Rahkonen [1]

[1] Circuits and Systems Research Unit (CAS), Faculty of ITEE, University of Oulu, Oulu, Finland
[2] CWC-Radio Technologies, Faculty of ITEE, University of Oulu, Oulu, Finland
Email: ara.assim@oulu.fi (A.A.A.); aarno.parssinen@oulu.fi (A.P.); timo.rahkonen@oulu.fi (T.R.)
*Corresponding author

***Abstract*—Modern 6G transceivers operate in the sub-THz band (100-300 GHz). Due to the high operating frequencies, baseband processing becomes particularly challenging. 6G systems propose using these frequency bands to achieve higher data capacity, but handling multi-GHz wide baseband signals presents a technical challenge. The purpose of this work is to investigate the interference mechanisms in a complex-IF downconversion receiver that selects distinct channels, often referred to as Component Carriers (CC) for independent processing. It is anticipated that the majority of receivers in the future will have similar architectures, because state-of-the-art analog-to-digital converters cannot process signals above 2-3 GHz bandwidth. Hence, the wide baseband must be divided into multiple component carriers, each will be processed separately in the digital domain. The receiver example in this work consists of eight component carriers and the bandwidth is up to 8 GHz. Interference due to image frequencies and harmonic mixing was studied using a MATLAB-based mathematical model. The results were verified through circuit-level simulations using passive Metal–Oxide–Semiconductor (MOS) mixers implemented in 130-nm SiGe BiCMOS technology, provided by the Leibniz Institute for High Performance Microelectronics (IHP) Solutions GmbH. Analog and digital mitigation techniques are described. Simulation results are provided for cancellation of harmonic mixing effects and cancellation of image frequency components in the digital domain. Image Rejection Ratio (IRR) improvement of about 10 dB was observed (from 25.5 dB to 35.6 dB), which is sufficient to detect the signal.**

***Keywords*—6G, co-channel interference, complex mixers, component carriers, harmonic mixing, image rejection ratio, THz receiver**

I. Introduction

In this paper, two interference mechanisms (image frequencies and harmonic mixing) are studied in a multiple carrier complex-IF receiver architecture [1–3]. Let us assume we have eight channels or Component Carriers (CC) located at positive and negative frequencies of the complex baseband. Each of them carries information, as shown in Fig. 1.

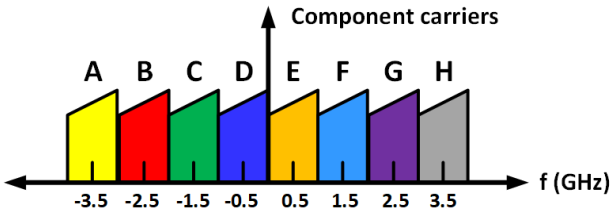

Fig. 1. Eight component carriers.

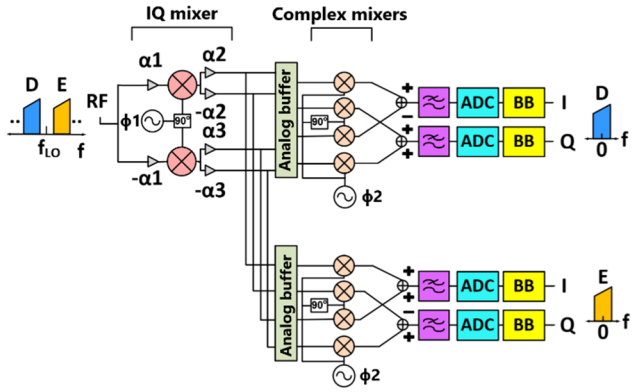

Fig. 2. The receiver architecture: An IQ downconversion stage followed by two complex mixers.

Fig. 2 shows the receiver architecture. The receiver starts with a traditional IQ downconversion mixer, it downconverts the eight CCs from the 300 GHz band to a complex-valued and very Broadband Baseband (BB) signal with a bandwidth of up to 8 GHz, having CCs A-D at negative and E-H at positive frequencies [4]. The downconversion may occur in a few steps, but for simplicity only one IQ mixer is shown.

Two analog buffers are placed after the IQ mixer, their purpose is to provide extra gain and drive the succeeding complex mixers with differential I and Q signals. Then each component carrier is further shifted to DC (0 Hz) by a complex downconversion mixer that can shift the complex spectrum to left or right. The outputs of the complex mixers are summed in the current domain using Transimpedance Amplifiers (TIAs).

Afterwards, they are separately filtered, digitized, and further processed, as illustrated for two channels in Fig. 2.

Manuscript received January 11, 2025; revised February 10, 2025, accepted February 24, 2025; published March 7, 2025.

The complex baseband signal is too broad to be digitized at one step, thus processing it continues in the analog domain.

There are two major interference mechanisms: image frequency, and harmonic mixing. The image is caused by mismatches in amplitude in the receiver's I/Q paths [5–7], and LO phases [8–10]. The amplitude mismatches of the mixers are labeled in Fig. 2 as α1, α2, and α3, while Local Oscillator (LO) phase mismatches are modeled as ϕ1 and ϕ2. The image appears as a mirrored replica of the channel from the opposite side of DC. For example: the mirrored and attenuated spectrum of channel D will appear on the top of channel E, when down converting channel E to DC in Fig. 1.

The magnitude of image signal and its dependence on the gain and phase mismatches were studied in more detail in [11]. The other issue is harmonic mixing [12–15]. Harmonic mixing is caused by the shape of mixing function, which is typically more nonlinear than the LO waveform itself. This is because the mixing transistors are usually hard driven on and off, as that maximizes the gain and minimizes their noise contribution. As an example, down converting channel E will also pick channels F and G, if the LO has 3rd and 5th harmonics [16]. The model above shows eight component carriers, and this makes harmonic mixing between the component carriers a major problem for the component carriers nearest to DC.

The paper is structured as follows: Section II illustrates the mixing artefacts, causes of image frequency and harmonic mixing issues, and a few analog techniques to minimize their effects. Section III describes a cancellation technique applied in the digital domain. A comparative analysis is presented in Section IV. Lastly, conclusions are made in Section V.

II. Mixing Artefacts

This section explains why image and harmonic mixing errors appear. As shown in Fig. 2, the receiver consists of a normal IQ downconverter, followed by two complex mixers. Each complex mixer shifts one channel (D or E in Fig. 2) to be centered at DC.

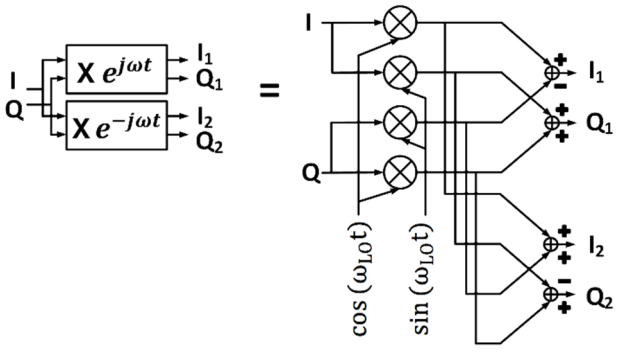

Fig. 3. Complex mixer: (a) complex mixing operation (b) complex mixer's structure.

Fig. 3 shows the structure of a complex mixer. Ideally, it can down convert the positive frequency component carrier to DC while cancelling the negative frequency carrier, or vice versa, depending on the order of the Local Oscillators (LO) fed.

However, the image rejection relies on the phase accuracy of the sine and cosine LOs, and the matching of the conversion gains of the mixers. The effects of I/Q mismatches on the complex mixer's IRR have been studied in Ref. [17, 18]. But in this work the Image-Rejection Ratio (IRR) analysis is more comprehensive as it considers all the nonidealities (amplitude and phase mismatches) of the complex mixer and the preceding IQ mixer.

The operation principle of a complex mixer is illustrated through Eqs. (1–4) [11], the following equations are derived from Fig. 3 (b):

$$I_1 = I\,cos(\omega_{LO}t) - Q\,sin(\omega_{LO}t) \quad (1)$$

$$Q_1 = I\,sin(\omega_{LO}t) + Q\,cos(\omega_{LO}t) \quad (2)$$

$$I_2 = I\,cos(\omega_{LO}t) + Q\,sin(\omega_{LO}t) \quad (3)$$

$$Q_2 = -I\,sin(\omega_{LO}t) + Q\,cos(\omega_{LO}t) \quad (4)$$

where I and Q are the inputs to the complex mixer that originate from a conventional IQ mixer. I_1, Q_1, I_2, and Q_2 are the differential outputs of the complex mixer.

Each of the outputs I_1, Q_1, I_2 and Q_2 are real signals, but they can be treated as a complex signal when they are measured differentially. Hence the phase information is preserved, and the corresponding image signal is canceled.

A. Image Frequency Issue and Image-Rejection Ratio (IRR)

I/Q mismatch can occur in quadrature mixers, resulting in leakage between the CCs when they are placed in the upper and lower sideband. The leaked CC that appears on the desired CC is known as image. This has been studied in Refs. [17–19]. The amount that the image signal is suppressed with respect to the wanted sign is expressed by the Image-Rejection Ratio (IRR) [20–22].

Different derivations of the IRR expression exist in literature, depending on the mixer architecture, parameters taken into account, and whether the IRR is considered frequency dependent or not. Broadly, IRR in an IQ mixer can be expressed as in Eq. (5) [21]:

$$IRR = \frac{Desired\ output\ signal}{Image\ signal} = \frac{(1+\varepsilon)^2 - 2(1+\varepsilon)\cos\theta + 1}{(1+\varepsilon)^2 + 2(1+\varepsilon)\cos\theta + 1} \quad (5)$$

where ε is the amplitude imbalance (mismatch), and θ is the phase imbalance.

An extensive frequency-independent IRR expression was derived in Ref. [11] for the receiver architecture in this work, it includes the amplitude and phase mismatches in the IQ mixer and complex mixer paths.

In general, a complex mixer is a bit less sensitive to image errors than a traditional IQ downconverter [11, 19]. In our design, the complex mixer's Image Rejection Ratio (IRR) is about 35.3 dB when phase error is 2 degrees. Gain

and offset trimming are commonly used in Gilbert cell type mixers. In this work, it is implemented by the bias adjustment of I and Q signal buffers.

The complex mixer is implemented with four passive MOS mixers. In such case, gain mismatches in the mixer path rise from mismatches in transistor sizes and threshold voltages, affecting the on resistance (R_{on}) of the pass transistor. Those can be mitigated by tuning a small series resistance before the mixer. Tuning the phase errors requires phase shifting in the LO path, which can be implemented by a controllable delay, if the LO is generated digitally.

B. Harmonic Mixing Issue and Analog Mitigation Techniques to Reduce it

Another problem is the mixing of harmonics. That has been a known problem, e.g., in cable TV, where the input spectrum is full of channels, so that picking one channel can pick a portion of the signal at an LO harmonic as well [23, 24].

3rd and 5th harmonic rejection have been studied in [13] for a 400-to-900 MHz receiver, but this work targets a higher frequency (up to 8 GHz).

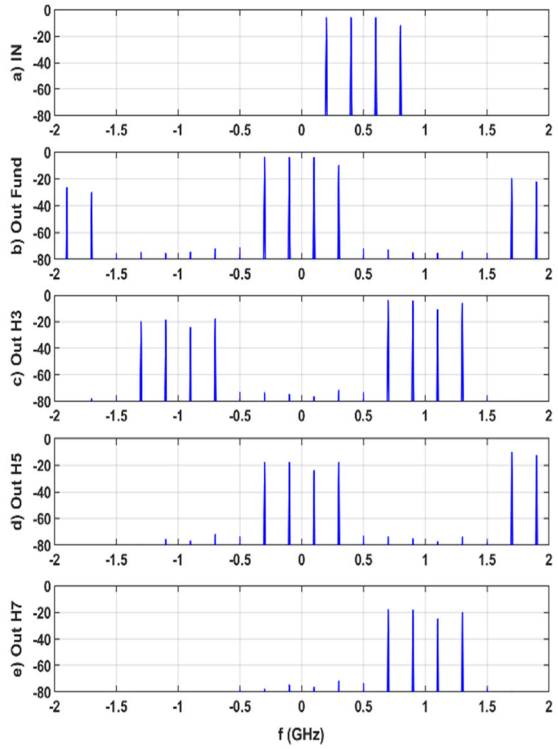

Fig. 4. Harmonic mixing in the complex mixer shifting the spectrum leftwards by 0.5 GHz and having harmonics at positive frequencies.

In the given receiver architecture, the harmonic mixing problem appears in the complex mixer stage. Harmonic mixing itself is not entirely dependent on the LO waveform, but on the waveform of the switched conductance: the LO can be strictly sinusoidal, but the on resistance of the switches still varies nonlinearly. Hence, the mixing function has harmonics and will mix down signal from the harmonics of the LO. If the mixing waveform is a square wave, the magnitude of the harmonics varies inversely proportional to the harmonic, so the 3rd harmonic is down by just –9.5 dB which is clearly excessive for OFDM channels needing an approximate value of 30 dB SNR.

Fig. 4 illustrates the harmonic mixing in a complex mixer, where the mixing function is 50% +/– switching, having 3rd, 5th, and 7th harmonic mixing gains of level –9.5, –14 and –16 dB, respectively.

Using the channel names shown in Fig. 1. Fig. 4 (a) shows the fundamental signal E now centered at a frequency of +0.5 GHz, and additional component carriers F, G, H will be added at the positive frequencies, centered to +1.5 GHz, +2.5 GHz, +3.5 GHz, one at a time. Fig. 4 (b) shows the signal E down converted to DC, and its 5th harmonic at –2 GHz. Fig. 4 (c) shows the mixing of channel F (centered at +1.5 GHz): fundamental mixing brings it harmlessly to +1 GHz and 5th harmonic mixing to –1 GHz. Fig. 4 (d) shows signal G falling as an interfering signal to DC by the 5th harmonic mixing. Lastly, Fig. 4 (e) shows that channel F mixing is again harmless for baseband reception of the desired channel E.

Above analysis showed that only the 5th harmonic mixing causes the interference to channel E at baseband when mixing leftwards and the interfering channels are at positive frequencies.

Subsequently, mixing rightwards is checked, that would bring channel D from –0.5 GHz to DC. Interferers F, G, and H are still added one by one at positive frequencies +1.5 GHz, +2.5 GHz, +3.5 GHz.

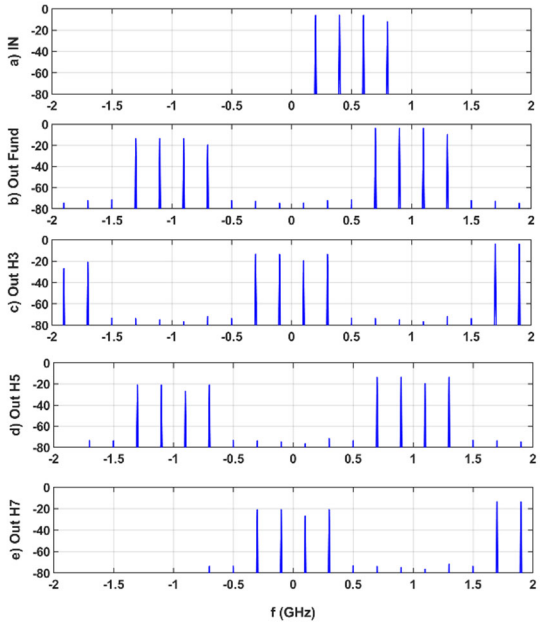

Fig. 5. Harmonic mixing in the complex mixer shifting the spectrum rightwards by 0.5 GHz and having harmonics at positive frequencies.

Fig. 5 shows similar response for a complex mixer converting rightwards. Now we see that 3rd harmonic mixing of F and 7th harmonic mixing of H both fall to DC where they interfere with the detection of the desired signal D from –0.5 GHz. Hence, 3rd and 7th harmonic mixing are seen to come from carriers from the other side of the DC, while the 5th harmonic mixing comes from the same side of origin. All of them are at a prominent level.

One technique to minimize the harmonic mixing is to make the multiplying waveform (which is by nature more nonlinear than the LO waveform) as sinusoidal as possible. In DSP implementation that is easily done e.g., by CORDIC generated sinusoids [25–27], but requires sampling of the entire band, which in this case is several GHz. One example of waveform tailoring in the analog domain is presented in [28, 29], where multiple parallel and binary weighted on/off mixers are combined to imitate a sinusoidal mixing waveform.

Something can also be done by tailoring the LO shape. In fully differential circuits the even harmonics are quite low by nature, so it is the odd harmonics that are problematic [30]. A trick commonly used in DC/AC inverters is to reduce the duty cycle of the +/–switching, and by varying the duty cycle between 30% and 40%, either 3rd or 5th harmonic can be cancelled. As shown in Fig. 6, the best combination appears at 36%, where 3rd and 5th harmonics are reduced to –24.89 dBc, and –11.69 dBc respectively compared to the fundamental harmonic. While 7th harmonic is much lower, hence not visible from the graph.

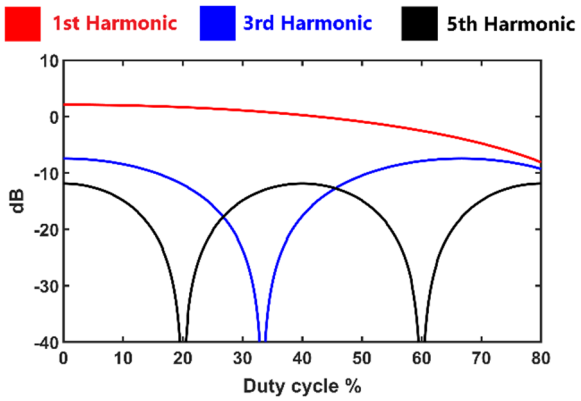

Fig. 6. Magnitude of the odd harmonics vs. LO signal's duty cycle.

Further improvement requires utilization of Harmonic Rejection Mixers (HRM). HRM implements multiple amplitude levels in the mixing function, i.e., multiple parallel switching mixers similar to [14, 28, 31].

RF transceivers frequently employ switching mixers due to numerous advantages over alternative mixer topologies [32]. Nevertheless, these mixers produce local oscillator frequency harmonics, which must be filtered. As an alternative, HRM can be used to reduce 3rd and 5th harmonics.

A HRM consists of three mixers connected in parallel, the center mixer has a gain of $\sqrt{2}$, as shown in Fig. 7 (a).

This gain of $\sqrt{2}$ can be obtained by adjusting the transconductance of the center mixer, or by scaling the sizes of the mixer transistors. In the given receiver, it is obtained by increasing the width of the transistors [31].

Three LO phases are needed (0°, 45°, 90°) to drive the Fig. 8 (c) and Fig. 8 (d) illustrate the effect of complex mixing. Ideally the complex mixer just moves the spectrum in Fig. 8 (b) leftwards or rightwards, but due to mismatches in the complex mixer, we will see signal c as image to signal d and vice versa. This means that when receiving signal, A, it is summed with a spectrally flipped (complex conjugated) channel B due to the IQ stage, and non-flipped signal B as an image of the complex mixer. In a similar manner, signal B is summed up by flipped and non-flipped spectrum of signal A.

mixers, and the outputs of the mixers are summed together. This results in a pseudo-sinusoidal LO function that significantly reduces 3rd and 5th harmonics, these effects are illustrated in Fig. 7 (b–c).

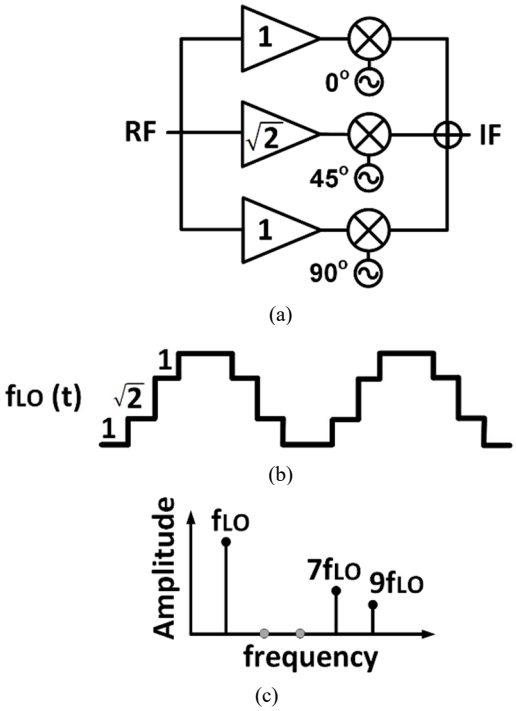

Fig. 7. Harmonic Rejection Mixer (HRM): (a) structure of a HRM (b) equivalent LO waveform (c) spectrum of the LO signal [31].

III. Digital Cancellation of the Interference

At the receiver's outputs, all the component carriers A-H will be available in the digital domain (although digitized by different analog-to-digital converters). This makes it possible to build a replica of the interference due to image signal or harmonic mixing and subtract it in the digital domain. In the following subsections, a few examples are shown on how that can be done.

A. Digital Cancellation of Image Signals

To be able to cancel the interfering signal, we need to know how the interference is generated and mimic that mechanism. Starting from the architecture shown in Fig. 2, we show how the image signal is formed and then use this information to cancel it.

The image signals are illustrated for a pair of channels in Fig. 8. To see the effect of the images, the signal should be plotted as two-sided spectrum and be treated as a complex envelope signal.

Fig. 8 (a) shows the IQ down conversion of a pair of channels, ending up as channels A and B in the complex baseband. Fig. 8 (b) shows the image generated in the IQ

down conversion: the image channel is flipped (complex conjugated) and falls on top of the desired channel.

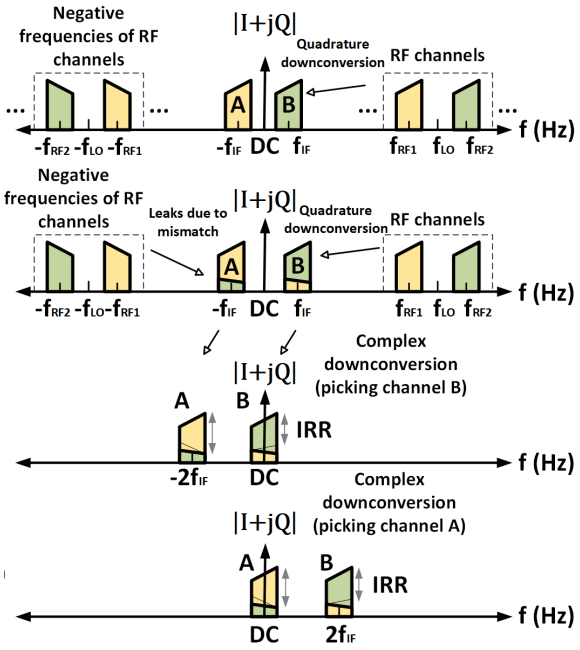

(a) (b) (c) (d)

Fig. 8. Illustration of image signal formation (a) Ideal down conversion of RF channels to IF (b) IQ down conversion with the effect of amplitude and phase mismatches (c) complex down conversion of channel B after IQ down conversion (d) complex down conversion of channel A after IQ down conversion.

Now that the interfering signals are known, a least squares method (LSM) adaption to subtract the interferers can be built. Eqs. (6) and (7) [19] explain how channels A and B are cleaned up from images.

$$A_{corrected} = A - c1.\ B - c3.\ B^* \tag{6}$$

$$B_{corrected} = B - c2.\ A - c4.\ A^* \tag{7}$$

where A, B, A∗, and B∗ indicate the desired channels and their conjugates, c1, ..., c4 are the coefficients used for the adaptation algorithm. Coefficients c1, ..., c4 are complex-valued coefficients that must be adapted. The normal recursive LSM adaptation works such that the coefficients are updated by a product of remaining error and the model function to be subtracted. If the original signal to interference ratio is good enough, we can use the uncorrected raw signals in Eqs. (6) and (7), but for better rejection the cleaned-up signals $A_{corrected}$, $B_{corrected}$ must be used as models for the image.

The correction was simulated by generating two pseudorandom QAM-modulated carriers, whose two-sided spectrum is shown in Fig. 9 (a). It is centered at 150 MHz and has a bandwidth of 30 MHz. The signal has a maximum amplitude of 2, its amplitude density function is given in Fig. 9 (b).

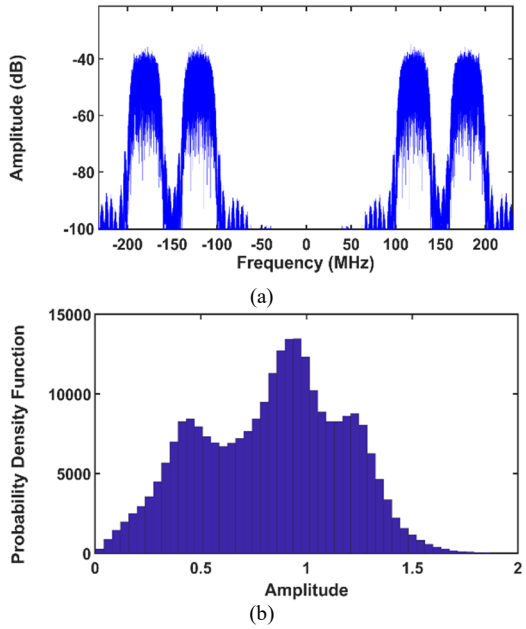

Fig. 9. The test RF signal (a) two-sided spectrum of the input RF signal (b) probability density function of the RF signal's amplitude.

Coefficients c1, ..., c4 were initialized to zero, and iteratively adapted every sample. Adaptation speed was chosen slow enough to converge.

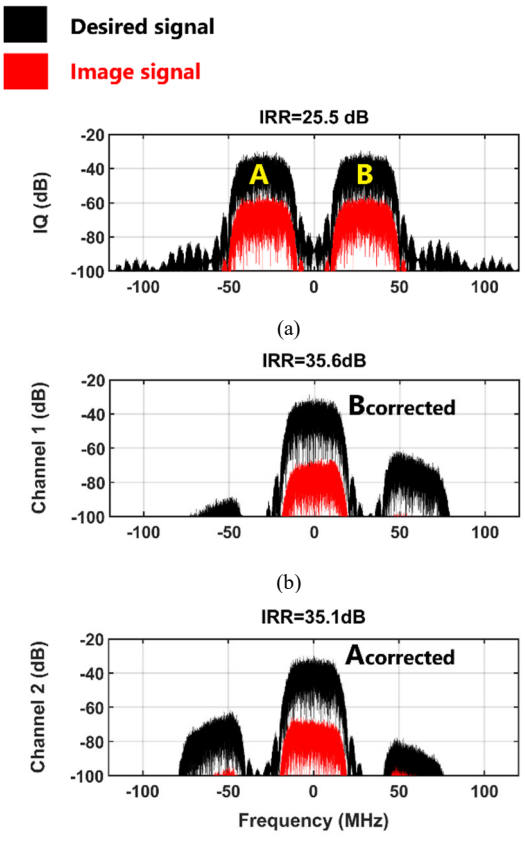

Fig. 10. Simulated spectral plot of (a) output of the IQ mixer (b) 1st output of the complex mixer after image correction (channel B) (c) 2nd output of the complex mixer after image correction (channel A).

Fig. 10 illustrates the process of adaptation, with Fig. 10 (a) showing the situation after the IQ down conversion. The simulation was repeated with and without mismatch errors so that the image error could be calculated: the desired signals are drawn in black, and the overlying image signals are in shown red. The ratio of the desired signal to the image signal is known as the image rejection ratio (IRR).

Existence of image frequencies make recognition of the signal harder, therefore most modern receivers require an IRR greater than 30 dB [33–36]. In this case, it is calculated simply as power ratios.

Fig. 10 (b–c) show the signals A and B after the complex mixer and error adaptation (Acorrected and Bcorrected). This experiment was mostly just proof of concept, but the original IRR of –25.5 dBc was improved to –35.6 dBc. This is already sufficiently high to allow QAM-64 modulation in the signal.

The adaptation of the coefficients in normal iterative LSM adaptation is illustrated for both channels in Fig. 11.

A higher adaptation rate was used until 10^5 samples, and then the adaptation was slowed down by a factor of 10.

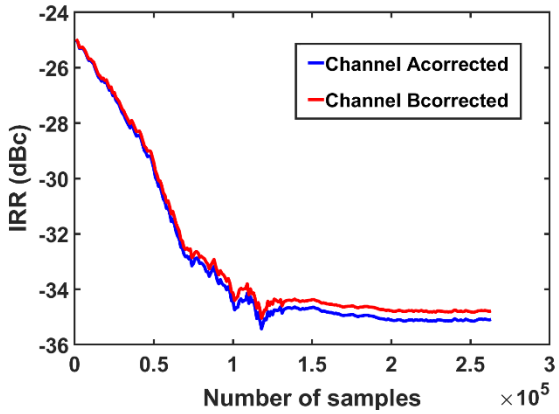

Fig. 11. Adaptation speed of the digital image rejection technique for channels Acorrected and Bcorrected.

B. *Digital Cancellation of Harmonic Mixing Effects*

Similar to image signals, how the interference is built up in harmonic mixing must be known. When harmonic mixing appears in the complex mixer, harmonics are picked alternatingly from positive and negative frequencies, as shown in Figs. 4–5.

Harmonic mixing only affects the channels D, E closest to DC, but the interference can be much stronger than those caused by images [37, 38]. As discussed above, to clean up signal E, signals D, F, and G must be available, then subtract them until correlation between the output and interferers disappears. This is provided in Eqs. (8), (9) [19].

$$D_{corrected} = D - c_1 . F - c_2 . B - c_3 . H \quad (8)$$

$$E_{corrected} = E - c_4 . C - c_5 . G - c_6 . A \quad (9)$$

Here the interferer is strong, but correction is unidirectional (the lowest channels are corrected in the harmonic mixing cancellation). For the image cancellation, correction was applied in both directions.

Fig. 12 shows the adaptation trajectory of the complex coefficients (c1, c2, c3, and c4), which were used in the adaptation algorithm in Eqs. (6–9). Coefficients c5 and c6 have rather little effect on the adaptation, hence they are not shown in Fig. 12.

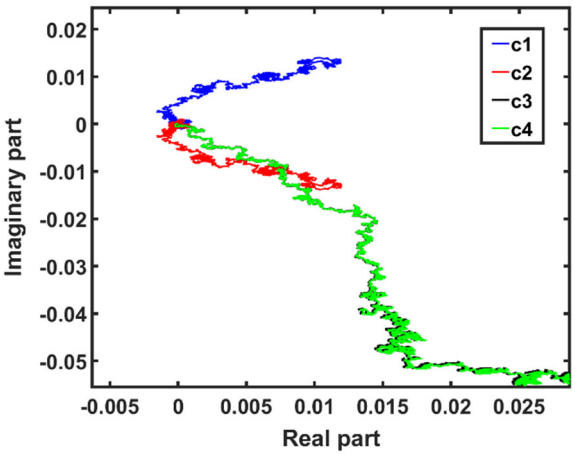

Fig. 12. Values of the adaptation coefficients c1, c2, c3 and c4 in cancellation of harmonic mixing effects.

The digital techniques are scalable to a larger number of channels (which is 8 in this article). However, the digital correction methods are not the limiting factor. There are other factors that limit the utilization of higher number of channels, including: maximum obtainable LO frequency, speed of the transistors, tolerable amount of harmonic mixing without using bulky IF filters, etc.

IV. Comparitive Analysis

Making a side-by-side comparison of the given receiver with prior works in literature is not a very straightforward task because each article had targeted a rather specific design approach with different circuit topologies, operating frequencies, and transistor technologies. Identical receiver designs which utilize complex mixers succeeding IQ mixers couldn't be found in literature.

In addition to that, the proposed receiver isn't completely ready. Certain parts have been designed, while the other parts are still in progress. Nonetheless, Table I compares this work with other works in literature that are deemed as similar as possible.

TABLE I. Comparison with Previous Works

Parameter	This work	[28]	[31]
Mixers in HRM	48	64	3
Component carriers	6-8	2	Not applicable
LO clock frequency	<4 GHz	390 MHz	86.4 MHz
Technology	130 nm SiGe	65 nm CMOS	350 nm CMOS
Correction domain	Analog & digital	Analog	Analog

V. Conclusion

This paper addresses the spurious responses in separating the component carriers from a very broadband complex baseband signal. The proposed architecture consists of traditional IQ down conversion, and then a complex mixer for moving each of the individual component carriers to DC. Image rejection in IQ mixers and complex mixers has been extensively researched, the latter are slightly less sensitive to gain and phase imbalances. However, harmonic mixing is a severe problem, as the highest harmonic mixing gain in the switching passive mixers is just -10 dB down the desired gain. Shaping the LO signal and employing multiple on/off mixers to imitate sinusoidal mixing are common solutions. It was found that asymmetrical harmonic mixing occurs from either the same or opposite side of the DC (depending on the harmonic). If the original signal is distinguishable, i.e., its SNR is not incredibly low due to image and harmonics, then it can be cleaned up from images and harmonic mixing in the digital domain. This is a novel area, because the imbalances in the IQ mixer cannot be corrected in a typical manner, since its outputs are not directly accessible, instead they are seen through the complex mixers. This work analyzed how the bands are flipped. The corresponding error model was built, along with a digital cancellation algorithm for cancelling both image frequency and harmonic mixing effects. Its LSM-based adaptation was checked. For image errors, it has demonstrated 10 dB improvement.

The cancellation studies of the harmonic mixing effects are currently under way.

Conflict of Interest

The authors declare no conflict of interest.

Author Contributions

Ara Abdulsatar Assim conducted the simulations at both circuit and system levels (using Cadence Virtuoso and MATLAB, respectively), analyzed the data, and wrote the manuscript; Aarno Pärssinen provided feedback and supervised the work; Timo Rahkonen supervised the work, provided the MATLAB code, and helped in preparing the manuscript; All authors had approved the final version.

Funding

This work was supported by 6G Flagship (Grant Number 369116) funded by the Research Council of Finland.

Acknowledgment

The authors would like to thank IHP GmbH for granting access to heterojunction bipolar transistor (HBT) technology.

References

[1] H. Li, "Interference mitigation in joint communications and sensing-part II: Coding and spreading," in *Proc. 2023 IEEE 3rd International Symposium on Joint Communications & Sensing (JC&S)*, Seefeld, Austria, 2023, pp. 1-6. doi: 10.1109/JCS57290.2023.10107466.

[2] C. S. Park, L. Sundström, A. Wallén and A. Khayrallah, "Carrier aggregation for LTE-advanced: Design challenges of terminals," *IEEE Communications Magazine*, vol. 51, no. 12, pp. 76–84, December 2013. doi: 10.1109/MCOM.2013.6685761.

[3] C. G. Tsinos, F. Foukalas, T. Khattab and L. Lai, "On channel selection for carrier aggregation systems," *IEEE Transactions on Communications*, vol. 66, no. 2, pp. 808–818, Feb. 2018. doi: 10.1109/TCOMM.2017.2757478.

[4] R. Chen and H. Hashemi, "Reconfigurable receiver with radio-frequency current-mode complex signal processing supporting carrier aggregation," *IEEE Journal of Solid-State Circuits*, vol. 50, no. 12, pp. 3032–3046, Dec. 2015. doi: 10.1109/JSSC.2015.2458971.

[5] S. C. Hwu and B. Razavi, "An RF receiver for intra-band carrier aggregation," *IEEE Journal of Solid-State Circuits*, vol. 50, no. 4, pp. 946–961, April 2015. doi: 10.1109/JSSC.2014.2386895.

[6] C. J. Lee, C. L. Tu, and S. J. Jou, "Online self-adaptive estimation and compensation design for dc voltage offset, frequency-independent, and frequency-Dependent IQ mismatch in sub-THz digital baseband transceiver," in *Proc 2024 IEEE International Symposium on Circuits and Systems (ISCAS)*, Singapore, Singapore, 2024, pp. 1–5. doi: 10.1109/ISCAS58744.2024.10558616.

[7] H. Yao, Y. Xiang, Y. Chen, C. Wang and J. Wu, "A wideband receiver I/Q mismatch calibration method in FDD transceiver," in *Proc. 2023 IEEE International Symposium on Circuits and Systems (ISCAS*), Monterey, CA, USA, 2023, pp. 1–4. doi: 10.1109/ISCAS46773.2023.10181489.

[8] F. Bozorgi, P. Sen, A. N. Barreto and G. Fettweis, "RF front-end challenges for joint communication and radar sensing," in *Proc 2021 1st IEEE International Online Symposium on Joint Communications and Sensing (JC&S)*, Dresden, Germany, 2021, pp. 1-6. doi: 10.1109/JCS52304.2021.9376387.

[9] N. G. Doan, H. C. Liu, C. W. Jen, and S. J. Jou, "Digital self-healing using smart sensing technique for IQ mismatch and LO leakage against non-flat path response in mmWave communication system," in *Proc. 2020 IEEE International Symposium on Circuits and Systems (ISCAS)*, Seville, Spain, 2020, pp. 1–5. doi: 10.1109/ISCAS45731.2020.9181271.

[10] X. R. Ma, D. D. Peng, Z. C. Ding, and X. Yao, "Compensation for transceiver IQ mismatch with phase noise in CO-OFDM system," in *Proc. 2016 15th International Conference on Optical Communications and Networks (ICOCN)*, Hangzhou, China, 2016, pp. 1–4. doi: 10.1109/ICOCN.2016.7875845.

[11] A. A. Assim, A. Parssinen and T. Rahkonen, "Using analog complex mixers for low-IF mixing," in *Proc. 2023 International Symposium on Fundamentals of Electrical Engineering (ISFEE),* Bucharest, Romania, 2023, pp. 1–6. doi: 10.1109/ISFEE60884.2023.10637096.

[12] S. Subhan, E. A. M. Klumperink, A. Ghaffari, G. J. M. Wienk, and B. Nauta, "A 100–800 MHz 8-Path polyphase transmitter with mixer duty-cycle control achieving <−40 dBc for all harmonics," *IEEE Journal of Solid-State Circuits*, vol. 49, no. 3, pp. 595–607, March 2014. doi: 10.1109/JSSC.2013.2297410.

[13] N. A. Moseley, Z. Ru, E. A. M. Klumperink, and B. Nauta, "A 400-to-900 MHz receiver with dual-domain harmonic rejection exploiting adaptive interference cancellation," in *Proc. 2009 IEEE International Solid-State Circuits Conference - Digest of Technical Papers*, San Francisco, CA, USA, 2009, pp. 232-233. doi: 10.1109/ISSCC.2009.4977393.

[14] S. Araei and N. Reiskarimian, "Implementation and application of harmonic reset switching in passive mixers," *IEEE Journal of Solid-State Circuits*, vol. 59, no. 12, pp. 4009–4021, Dec. 2024. doi: 10.1109/JSSC.2024.3462296.

[15] V. Singh, T. Forbes, W. G. Ho, J. Ko, and R. Gharpurey, "A 16-band channelizer employing harmonic rejection mixers with enhanced image rejection," in *Proc. IEEE 2014 Custom Integrated Circuits Conference*, San Jose, CA, USA, 2014, pp. 1–4. doi: 10.1109/CICC.2014.6946013.

[16] A. Ahmed and G. M. Rebeiz, "An 8–30 GHz high-linearity harmonic-rejection mixer in 45 nm CMOS SOI," I*EEE Transactions on Microwave Theory and Techniques*, vol. 72, no. 6, pp. 3361–3372, June 2024. doi: 10.1109/TMTT.2023.3327884.

[17] P. I. Mak, S. U. Pan, and R. P. Martins, "A front-to-back-end modeling of I/Q mismatch effects in a complex-IF receiver for image-rejection enhancement," in *Proc. 10th IEEE International Conference on Electronics, Circuits and Systems*, 2003, pp. 631–634, vol. 2. doi: 10.1109/ICECS.2003.1301864.

[18] L. R. Wilhelmsson, J. Svensson, M. Anderson, S. Ek, R. Strandberg, and L. Sundstrom, "Design of a configurable complex IF receiver supporting LTE carrier aggregation," in *Proc. 2013 IEEE 77th Vehicular Technology Conference (VTC Spring)*, Dresden, Germany, 2013, pp. 1–5. doi: 10.1109/VTCSpring.2013.6692505.

[19] A. A. Assim, A. Pärssinen, and T. Rahkonen, "Modeling image signal and its cancellation in complex downconversion circuit," in *Proc. 15th international conference on Scientific Computing in Electrical Engineering (SCEE)*, Darmstadt, Germany, 2024.

[20] C. W. Byeon, J. H. Lee, D. Y. Lee, M. R. Kim, and J. H. Son, "A high linearity, image/LO-rejection I/Q up-conversion mixer for 5G cellular communications," in *Proc. 2015 10th European Microwave Integrated Circuits Conference (EuMIC)*, Paris, France, 2015, pp. 345–348. doi: 10.1109/EuMIC.2015.7345140.

[21] W. H. Lin, H. Y. Yang, J. H. Tsai, T. W. Huang, and H. Wang, "1024-QAM high image rejection E-band sub-harmonic IQ modulator and transmitter in 65-nm CMOS process," *IEEE Transactions on Microwave Theory and Techniques*, vol. 61, no. 11, pp. 3974–3985, Nov. 2013. doi: 10.1109/TMTT.2013.2284473.

[22] D. Varun and G. R. Kadambi, "Mixer architecture with improved image rejection and interference mitigation for cognitive radio," in *Proc. 2016 IEEE Annual India Conference (INDICON)*, Bangalore, India, 2016, pp. 1–5. doi: 10.1109/INDICON.2016.7839047.

[23] H. Zhang, T. B. Gao, S. C. G. Tan and O. Shana'a, "A harmonic-rejection mixer with improved design algorithm for broadband TV tuners," in *Proc. 2012 IEEE Radio Frequency Integrated Circuits Symposium*, Montreal, QC, Canada, 2012, pp. 163–166. doi: 10.1109/RFIC.2012.6242255.

[24] C. Chen, J. Wu, C. Huang, and L. Shi, "A CMOS switched load harmonic rejection mixer for DTV tuner applications," *IEEE Transactions on Circuits and Systems I: Regular Papers*, vol. 60, no. 2, pp. 428–436, Feb. 2013. doi: 10.1109/TCSI.2012.2215695.

[25] P. K. Meher, J. Valls, T. B. Juang, K. Sridharan, and K. Maharatna, "50 years of CORDIC: Algorithms, architectures, and applications," *IEEE Transactions on Circuits and Systems I: Regular Papers*, vol. 56, no. 9, pp. 1893–1907, Sept. 2009. doi: 10.1109/TCSI.2009.2025803.

[26] M. Garrido, P. Källström, M. Kumm, and O. Gustafsson, "CORDIC II: A new improved cordic algorithm," *IEEE Transactions on Circuits and Systems II: Express Briefs*, vol. 63, no. 2, pp. 186–190, Feb. 2016. doi: 10.1109/TCSII.2015.2483422.

[27] N. Hou, M. Wang, X. Zou, and M. Liu, "A low latency floating point CORDIC algorithm for sin/cosine function," in *Proc. 2019 IEEE 4th International Conference on Signal and Image Processing* (ICSIP), Wuxi, China, 2019, pp. 751–755. doi: 10.1109/SIPROCESS.2019.8868623.

[28] L. Sundström *et al*., "Complex IF harmonic rejection mixer for non-contiguous dual carrier reception in 65 nm CMOS," in *Proc. 2012 Proceedings of the ESSCIRC (ESSCIRC)*, Bordeaux, France, 2012, pp. 357–360. doi: 10.1109/ESSCIRC.2012.6341328.

[29] S. Ibrahim *et al*., "Wideband tunable N-Path Mixer with calibrated harmonic rejection including the 7th LO harmonic," *IEEE Transactions on Circuits and Systems I: Regular Papers*, vol. 71, no. 9, pp. 3939–3950, Sept. 2024. doi: 10.1109/TCSI.2024.3414183.

[30] N. Shams and F. Nabki, "Analysis and comparison of low-power 6-GHz N-path-filter-based harmonic selection RF receiver front-end architectures," *IEEE Transactions on Very Large-Scale Integration (VLSI) Systems*, vol. 30, no. 3, pp. 253–266, March 2022. doi: 10.1109/TVLSI.2022.3142235.

[31] J. A. Weldon *et al*., "A 1.75-GHz highly integrated narrow-band CMOS transmitter with harmonic-rejection mixers," *IEEE Journal of Solid-State Circuits*, vol. 36, no. 12, pp. 2003–2015, Dec. 2001. doi: 10.1109/4.972151.

[32] M. T. Terrovitis and R. G. Meyer, "Noise in current-commutating CMOS mixers," *IEEE Journal of Solid-State Circuits*, vol. 34, no. 6, pp. 772–783, June 1999. doi: 10.1109/4.766811.

[33] L. Sundström, M. Anderson, M. Andersson, and P. Andreani, "Harmonic rejection mixer at ADC input for complex IF dual carrier receiver architecture," in *Proc. 2012 IEEE Radio Frequency Integrated Circuits Symposium*, Montreal, QC, Canada, 2012, pp. 265–268. doi: 10.1109/RFIC.2012.6242278.

[34] L. Gao, Q. Ma, and G. M. Rebeiz, "A 20–44-GHz image-rejection receiver with >75-dB image-rejection ratio in 22-nm CMOS FD-SOI for 5G applications," *IEEE Transactions on Microwave Theory and Techniques*, vol. 68, no. 7, pp. 2823–2832, July 2020. doi: 10.1109/TMTT.2020.2979441.

[35] S. Kawai *et al*., "A 1024-QAM capable WLAN receiver with −56.3 dB image rejection ratio using self-calibration technique," in *Proc. 2017 IEEE International Symposium on Circuits and Systems (ISCAS)*, Baltimore, MD, USA, 2017, pp. 1–4. doi: 10.1109/ISCAS.2017.8050600.

[36] H. Duan, Q. Chen, X. Wu, D. Wang, L. Li, and X. You, "A multi-band and high-IRR down-conversion mixer for 5G NR FR2 using compact transformer-based mutual-image-rejection filter," in *Proc. 2024 IEEE Radio Frequency Integrated Circuits Symposium (RFIC)*, Washington, DC, USA, 2024, pp. 323–326. doi: 10.1109/RFIC61187.2024.10599992.

[37] N. Guler, "Vertical handover-based hybrid RF/VLC scheme for e-health applications (VHO-HeA)," *Engineered Science*, 2024. doi: 10.30919/es1252.

[38] N. Guler and M. Salamah, "ARCH: Adaptive resource allocation for cooperative transmission in hybrid SWIPT-enabled wireless powered sensor networks," *Engineered Science*, Jan. 2023, doi: 10.30919/es932.